Photoemission from Xe in the vicinity of the 4d Cooper minimum

D. W. Lindle,* T. A. Ferrett,* P. A. Heimann,† and D. A. Shirley
Materials and Chemical Sciences Division, Lawrence Berkeley Laboratory,
University of California, Berkeley, California 94720
and Department of Chemistry, University of California, Berkeley, California 94720
(Received 17 September 1987)

Partial photoionization cross sections and angular-distribution asymmetry parameters have been determined for the Xe 4*d* and "4*p*" subshells in the photon-energy region of the 4*d* Cooper minimum (160 eV to 270 eV, to 520 eV for the 4*d* asymmetry parameter). The Cooper minimum is observed as a distinct cross-section minimum in the 4*d* photoionization channel. The 4*d* angular-distribution results are in excellent agreement with Dirac-Fock and relativistic random-phase-approximation calculations and with previous measurements. Effects of interchannel coupling are evident in the "4*p*" results. Both the partial cross section and the angular distribution for the "4*p*" photoelectron peak track the 4*d* cross section and angular distribution as functions of photon energy. A similar result is observed for the summed intensity and the angular distribution of the $4d^{-1}5p^{-1}np$ satellites of the 4*d* main line, which is probably due to the effects of electron correlation between the 4*d* and the satellite photoionization channels.

I. INTRODUCTION

Inner-shell photoemission experiments on Xe have been used to study one-electron and multielectron effects in atomic photoionization.[1–22] For example, photoemission from the Xe 4*d* subshell has shown that a series of single-electron processes combines to produce oscillations in both the subshell cross section[5,6,10,11,15,16,19–22] and the angular-distribution asymmetry parameter[4,8,14,15,21,22] over a wide range of photon energies beginning just above threshold. The lack of important many-electron effects on the 4*d* parameters can be attributed, in part, to the fact that the 4*d* photoemission channel dominates the absorption cross section for the Xe atom.[5,11–13] By the same token, photoemission from other subshells in Xe, such as 5*s* and 5*p*, exhibits strong many-electron effects, due to interchannel coupling with the 4*d* subshell.[20] For both of the valence subshells in Xe, changes in the partial cross section[3] [and the asymmetry parameter for 5*p* (Refs. 7 and 9)] have been observed and identified as results of coupling to the stronger 4*d* channel.

At photon energies immediately above the 4*d* ionization threshold, the photoelectron spectrum is dominated by features associated with 4*d*-vacancy states. It is known[8,15,20] that photoemission from the 4*d* subshell beyond a few eV above threshold can be described accurately by the following series of one-electron effects in the $4d \rightarrow \epsilon f$ continuum channel: a rapid change in the Coulomb phase shift occurs closest to threshold, followed at somewhat higher energy by a centrifugal-barrier-shape resonance,[12,13,23] and finally, at still higher energy, the $4d \rightarrow \epsilon f$ dipole matrix element experiences a change in sign which causes a "Cooper minimum" in the cross section.[24] Experimentally, pronounced changes have been observed in the absorption cross section,[25–29] the 4*d* partial cross section,[5] the spin-orbit branching ratio,[6] and the angular distribution of Xe 4*d* photoelectrons.[4,8] However, most of these earlier measurements, with one exception,[8] have focused on the energy region below the 4*d* Cooper minimum. The present work addresses the effects on 4*d* photoemission in the region of the Cooper minimum. The 4*d* partial cross section has been measured for the first time through the Cooper minimum, and new results for the 4*d* asymmetry parameter also are presented. They improve significantly our earlier measurements,[8] and extend the angular-distribution results to higher energy (520-eV photon energy). Excellent agreement is observed with theoretical calculations[15,21,22] of these primarily one-electron effects.

New results for the Xe "4*p*" photoionization channel are presented here as well. We use quotes for the "4*p*" channel to signify that the $Xe^{+}(4p^{-1})$ ionic state does not exist *per se*, but mixes strongly with many other single-ion final states (e.g., $4d^{8}nl$).[18] The present results indicate that the "4*p*" peak mimics the behavior of the 4*d* subshell throughout the photon-energy range of this work (185–270 eV). Single-electron calculations[15] fail to predict this behavior, which is found to be quite similar to previous measurements[30] of isoelectronic I (in CH_3I). In the I "4*p*" experiment, a tentative explanation was put forth in which the importance of the configuration $4d^{8}4f$ to the ionic state reached by "4*p*" ionization comes into play. It was suggested that one could regard the $4d^{8}4f$ state as being a correlation satellite of the stronger 4*d* peak. In the present work, we discuss, in addition, the possibility of interchannel coupling between the 4*d* and "4*p*" channels, which can be viewed as being similar to the coupling between the 4*d* and the valence subshells (5*s* and 5*p*) of Xe. For the valence subshells, experimental observations[3,7,9] illustrate that both peaks exhibit effects due to interchannel coupling in the photon-energy range of the $(4d \rightarrow \epsilon f)$-shape resonance ($\sim 100$ eV).

A brief description of the experimental technique is given in Sec. II. The 4d and "4p" subshell results are presented in Sec. III, and conclusions are discussed in Sec. IV.

II. EXPERIMENT

The experiment was performed at the Stanford Synchrotron Radiation Laboratory with the same time-of-flight (TOF) apparatus[31] and experimental conditions that were used in the previous work on CH_3I (Ref. 30) and Kr.[32] The monochromator resolution for the Xe experiment was a constant 1.3 Å at all photon energies.

For photoionization of a randomly oriented sample by linearly polarized radiation, Yang's theorem[33] defines the differential cross section in the dipole approximation as

$$\frac{d\sigma(h\nu,\theta)}{d\Omega}=\frac{\sigma(h\nu)}{4\pi}[1+\beta(h\nu)P_2(\cos\theta)] . \quad (1)$$

In Eq. (1), θ is the angle between the momentum vector of the ejected electron and the polarization vector of the ionizing radiation, $P_2(\cos\theta)$ is the second Legendre polynomial, and $\sigma(h\nu)$ and $\beta(h\nu)$ are the cross section and asymmetry parameter, respectively, for the photoionization process under study. Cross sections and asymmetry parameters are derived from photoelectron spectra taken with $\theta=0°$ and $\theta=54.7°$, as described in previous publications.[30,32] At certain photon-energy settings of the monochromator, second-order radiation (i.e., $2h\nu$) was sufficiently intense to produce peaks in our spectra, mostly second-order peaks from Xe 4d ionization. Consequently, the 4d asymmetry-parameter results were extended to higher photon energy.

In the photon-energy range of the Xe experiment, it has been determined[34] that the scintillator sodium salicylate, which we use to measure the relative photon flux, has a monotonically increasing efficiency. Therefore it was necessary to correct our relative cross-section measurements by as much as 50%. As a result, the usually quoted systematic errors of ±10% for our relative cross sections become ±20% in the high-energy region of the present measurements. The branching-ratio and asymmetry-parameter results, which are independent of the photon-flux measurement, have estimated systematic errors of ±10% and ±0.1, respectively. The estimated systematic errors are not included in the error bars of the data presented in this work.

III. RESULTS AND DISCUSSION

A TOF photoelectron spectrum of Xe taken at 250 eV photon energy is shown in Fig. 1. This spectrum contains the unresolved $4d_{5/2}$ and $4d_{3/2}$ photoemission lines with binding energies of 67.5 and 69.5 eV, respectively. We also observe the "4p" peak [binding energy, 145.5 eV (Ref. 1)] and an accompanying Coster-Kronig $N_{2,3}N_{4,5}O_{2,3}$ Auger feature near 50 eV kinetic energy. The enhanced intensity on the low-kinetic-energy side of the "4p" peak consists of many lines ($4d^8nl$) and some continuum-like structure ($4d^8\epsilon l$). Higher-resolution x-ray photoelectron spectra of this kinetic energy region

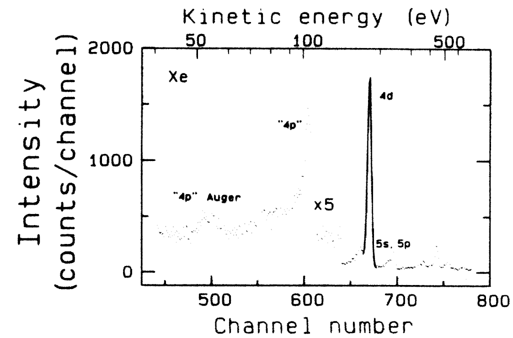

FIG. 1. TOF photoelectron spectrum of Xe at 250 eV photon energy and with $\theta=54.7°$. The peaks at high kinetic energy result from photoionization by higher-order radiation from the monochromator.

can be found in Refs. 1 and 2. The remaining high-energy peaks result from photoionization of the valence subshells and from photoemission induced by higher-order radiation from the monochromator.

A. 4d subshell

The 4d cross-section results are shown in the top portion of Fig. 2. All of the present cross-section measurements are given in arbitrary units, because of the lack of available quantitative information in the 160–270 eV photon-energy range. For example, we are unable to scale our relative peak intensities to the total absorption cross section[29] without further knowledge of the importance of direct multiple ionization. While there is evidence[11] that a considerable fraction of the total cross section above 100 eV photon energy results from double ionization, there are no available quantitative measurements of this fraction. In addition, we were unable to determine quantitatively the relative intensity of the higher-binding-energy continuumlike structure to the left of the "4p" peak in Fig. 1. Finally, although there exist[11] 4d cross-section results on an absolute scale up to 160 eV, the overlap with the present work is insufficient to reliably scale our results. Thus we report only relative cross sections.

The 4d cross-section data shown in the top of Fig. 2 exhibit a clear minimum which can be attributed to a Cooper minimum[24] in the $4d\rightarrow\epsilon f$ photoemission channel. The rise to lower energies in Fig. 2 corresponds to the high-energy side of the prominent ($4d\rightarrow\epsilon f$)-shape resonance[12,13,23] that has been well characterized in Xe. At higher photon energies, σ_{4d} recovers by more than a factor of 2 from its minimum value. The position of the Cooper minimum is 185(10) eV, in excellent agreement with absorption spectra.[25–29]

The Xe 4d asymmetry-parameter results are shown in the bottom portion of Fig. 2, and over a wider photon-energy range in Fig. 3. Also included in these figures are previous measurements[4,8] of β_{4d} and several theoretical curves.[15,21,22] The experiments are in excellent agreement with each other and with the two relativistic calculations.[21,22] The Dirac-Fock (DF)[21] and relativistic

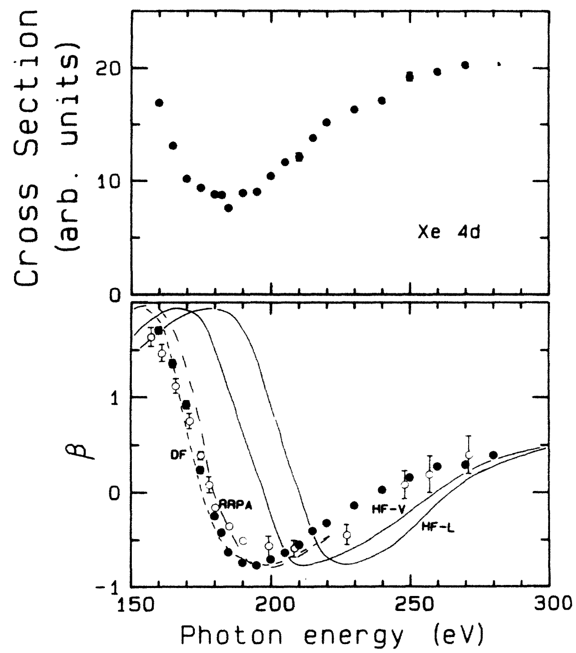

FIG. 2. Partial cross section (top) and asymmetry parameter (bottom) of the Xe 4*d* subshell. The experimental measurements are from the present work (closed symbols) and from Ref. 8 (open symbols). The theoretical curves in the bottom panel are from Refs. 21 (DF), 22 (RRPA), and 15 (HF-*V*, HF-*L*).

random-phase-approximation (RRPA)[22] calculations predict the rapid decrease of β_{4d} at low energy, which is due to the Cooper minimum. The nonrelativistic Hartree-Fock [HF-*V* (velocity) and HF-*L* (length)] calculations[15] predict the correct shape of β_{4d}, including the asymptotic value at high energy, but miss the energy of the Cooper minimum by 20–30 eV. The present results are in better agreement with theory at the minimum in β_{4d}. These new results are to be preferred over our earlier measurements[8] in the regions of overlap, based on improved accuracy.

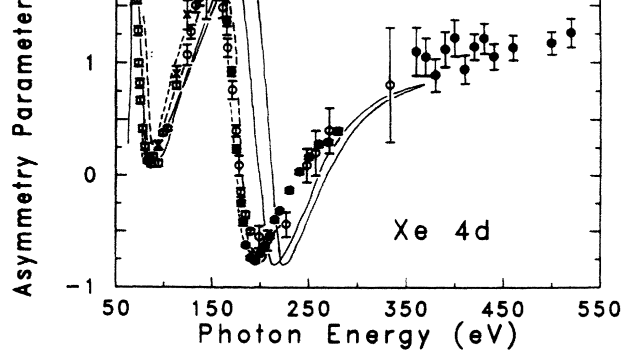

FIG. 3. Assymetry parameter of the Xe 4*d* subshell as in the bottom panel of Fig. 2, now including experimental results from Ref. 4 (×), plotted over a wider photon-energy range.

Using the expression for β in *jj* coupling (Ref. 35), β_{4d} is predicted to be approximately 0.2 at the Cooper minimum. This value for β_{4d} is reached at a photon energy between 175 and 180 eV, in fairly good, but not exact, agreement with the 4*d* cross-section results.

At a few photon energies in the 160–182.5-eV range approaching the Cooper minimum, a 4*d* correlation satellite was resolved from the 4*d* photoemission main line (the satellite appears in Fig. 1 as a shoulder to the left of the 4*d* peak), allowing us to make a crude measurement of its intensity and angular distribution. This peak corresponds to the sum of the $4d^{-1}5p^{-1}np$ satellite states.[1] Qualitatively, the intensity of this satellite peak relative to the 4*d* main line was found to be roughly constant throughout this energy range. Quantitatively, we measured the relative intensity to be 12(3)%, in disagreement with previous measurements of the satellite-to-main-line ratio of 6(1)% at both 151 eV photon energy and at 1486 eV (Al $K\alpha$).[36] This discrepancy is probably explained by the poor kinetic energy resolution of the present measurements, and by the presence of a background underlying the satellite peak which arises from Auger decay of the ionic states produced in the "4*p*" binding-energy region. This background would not appear at either 151 or 1486 eV photon energy, because the satellite peak would be at a different kinetic energy than that of the underlying Auger electrons.

The asymmetry parameter for the sum of the $4d^{-1}5p^{-1}np$ satellites closely follows β_{4d} in this energy range, dropping from 1.4(2) at 160 eV to −0.6(2) at 182.5 eV. The present results indicate that the 4*d* correlation satellites seem to experience the Cooper minimum in the $4d \rightarrow \epsilon f$ channel at the same *photon* energy as the 4*d* main line. This is not expected in the conventional one-electron picture, in which the photoelectron's *kinetic* energy should determine the position of the Cooper minimum. However, in the presence of electron correlation, which clearly is important for satellite lines, this result is not necessarily so unexpected. In fact, similar, but more dramatic, effects have been observed for a satellite in the *S* 2*p* region of the molecule SF_6.[37]

B. "4*p*" subshell

Gelius[1] and Svensson *et al.*[2] recorded Al $K\alpha$ photoelectron spectra of Xe in the region of the 4*p* binding energies. Rather than finding two peaks ($4p_{3/2}$ and $4p_{1/2}$) corresponding to one-electron transitions to Xe^+, they found effects of multielectron behavior in the photoelectron spectrum. Wendin and Ohno[18] explained this phenomenon in Xe in terms of strong configuration mixing, which prevents the existence of an isolated $4p_{3/2}$- or $4p_{1/2}$-hole state, and requires that a "4*p*" vacancy appear primarily as $Xe^+(4d^84f)$. The strong coupling results from the near degeneracy of a single 4*p* hole and a double vacancy with two 4*d* holes. A similar description is based on the onset of $N_{2,3}N_{4,5}N_{4,5}$ (super-Coster-Kronig) Auger decay in the photon-energy range of Xe "4*p*" ionization. This ambiguity in the identification of the $4p^{-1}$ final state is reflected in our use of quotes in specifying the "4*p*" ionization channel. The mixed configuration identity of the "4p" line also is relevant to the "4p" Auger feature in Fig. 1. We can identify this peak as being related to either of the two processes, $Xe^{+}(4p^5) \rightarrow Xe^{+2}(4d^9 5p^5)$ or $Xe^{+}(4d^8 4f) \rightarrow Xe^{-2}(4d^9 5p^5)$, both of which yield Auger electrons of the appropriate energy.

The "4p" cross-section and asymmetry-parameter results for photon energies from 185 to 280 eV are shown in Fig. 4. These values were determined by considering only the area under the single prominent $(4d^8 4f)$ peak in Fig. 1 and excluding insofar as possible the continuumlike structure at lower kinetic energy. We will interpret the data in Fig. 4 as primarily representing the $4d^8 4f$ final state.

The Xe "4p" cross-section data in the top portion of Fig. 4 are on the same arbitrary scale as σ_{4d} in Fig. 2. The intensity of the $4d^8 4f$ peak accounts for less than half of the total intensity in the "4p" region, the remainder being in the broad continuum structure seen in Fig. 1. Thus, the cross section for all of the photoemission occurring in the "4p" binding-energy region is of the same order as σ_{4d} in the vicinity of the 4d Cooper minimum. Also in the top of Fig. 4 is a curve which represents a smooth function through the σ_{4d} results in the top of Fig. 2, divided by 4. From this comparison, we observe that the cross section of the "4p" peak varies with σ_{4d}, and possibly experiences the Cooper minimum in the $4d \rightarrow \epsilon f$ channel.

The "4p" asymmetry-parameter results in the bottom portion of Fig. 4 also exhibit behavior very similar to β_{4d}, which is represented by the solid curve in the bottom panel. Also included in this panel is a curve representing a HF-V calculation,[15] which predicts β_{4p} within a one-electron approximation. Clearly, the curve representing β_{4d} matches the "4p" results better than the HF-V curve. An identical observation has been made for $\beta_{\text{"}4p\text{"}}$ and β_{4d} for the I atom in CH_3I.[30]

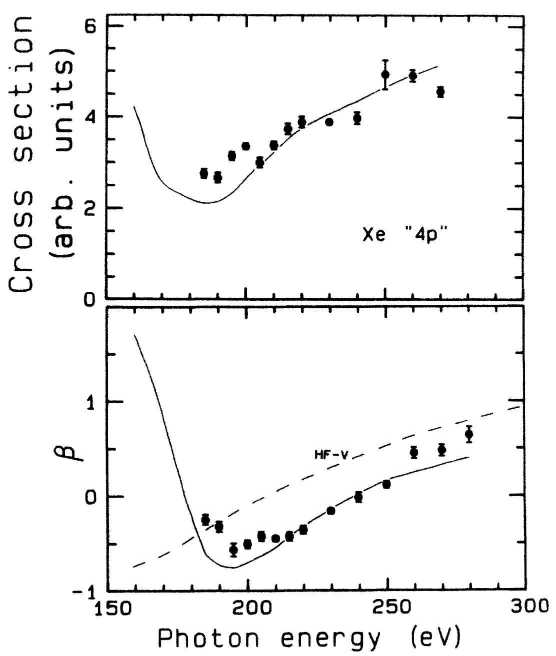

FIG. 4. Partial cross section (top) and asymmetry parameter (bottom) of the Xe "4p" $(4d^8 4f)$ photoelectron peak. The cross section is on the same arbitrary scale as that of σ_{4d} in the top panel of Fig. 2. The solid curves represent the σ_{4d} (divided by 4) and β_{4d} data in Fig. 2, and the dashed curve represents a HF-V calculation of β_{4p} (Ref. 15).

The similarities between the measured parameters for the Xe "4p" and 4d subshells are striking. In the work on CH_3I,[30] recourse was made to the identification of the "4p" peak with the $4d^8 4f$ configuration in order to liken the "4p" peak to a correlation satellite of the $4d^9$ main-line final state. Therefore, the "4p" peak may be considered to be derived from the 4d main line, and thus might be expected to mimic the 4d behavior as a function of energy. However, there are two problems with this picture. First, the binding-energy difference between the $4d^8 4f$ and $4d^9$ ionic states is large ($\sim$70 eV), suggesting that the large difference in kinetic energies of the 4d and "4p" photoelectrons may lead to different cross sections and angular distributions as a function of photon energy (kinetic energy effect). Second, the $4d^8 4f$ state that is designated as a satellite would correspond heuristically to a $4d \rightarrow 4f$ excitation accompanying 4d ionization, which is similar to a "conjugate shake-up" satellite because of the change in the orbital angular momentum of the excited electron. Generally, such satellites are expected to behave differently than their main lines.[38]

While the description of the "4p" peak as a satellite of the 4d line is possible, there is a different picture within which to discuss the observed similarities for the 4d and "4p" data. It is known that interchannel coupling with the 4d continuum plays an important role for the Xe valence shell. At photon energies near the $(4d \rightarrow \epsilon f)$-shape resonance, the 5s and 5p subshells exhibit enhancement[3] which has been attributed to coupling with the 4d channel.[20] Similarly, if the 4d channel were to couple with the "4p" subshell, one might expect the "4p" cross section and asymmetry parameter to exhibit effects of this coupling. The exact mechanism by which the 4d and the $4d^8 4f$ photoemission channels could couple through the continuum and lead to the same spectral shape for their cross sections and asymmetry parameters requires further theoretical understanding. In addition, the extent to which the $4d^8 4f$ configuration, identified with the "4p" peak, plays the role of a satellite of the 4d line, is unknown, and needs to be determined with a dynamical calculation that properly treats the many-electron nature of the "4p" region of the Xe spectrum.

IV. CONCLUSIONS

Inner-shell photoemission from Xe in the vicinity of the 4d Cooper minimum has been reported. The new results for σ_{4d} and β_{4d} illustrate dramatic effects due to the zero in the $4d \rightarrow \epsilon f$ transition amplitude. We observe excellent agreement with previous measurements and with relativistic calculations which treat 4d ionization in a single-electron framework.

In contrast, many-electron effects appear to be important for describing photoionization of both the "4p" subshell and the $4d^{-1}5p^{-1}np$ satellites of the 4d main line. The results for each of these photoemission channels resemble σ_{4d} and β_{4d} throughout the energy range of the 4d Cooper minimum, suggesting the possibility of strong interchannel coupling and main-line–satellite interactions, or possibly a combination of both effects for "4p" ionization. This general picture of the importance of many-electron effects tied to the 4d subshell seems to be valid even though the 4d channel is experiencing a minimum in this energy range, and thus does not dominate the photoionization process. Further theoretical work is needed to clarify the coupling by which the 4d photoemission process exerts such an influence over the other Xe photoionization channels in this energy range.

ACKNOWLEDGMENTS

The authors wish to thank S. T. Manson for helpful discussions. This work was supported by the Director, Office of Energy Research, Office of Basic Energy Sciences, Chemical Sciences Division of the U. S. Department of Energy under Contract No. DE-AC03-76SF00098. It was performed at the Stanford Synchrotron Radiation Laboratory, which is supported by the Department of Energy's Office of Basic Energy Sciences.

*Present address: National Bureau of Standards, Gaithersburg, MD 20899.

†Present address: Technische Universität München, D-8046 Garching bei München, West Germany.

[1]U. Gelius, J. Electron Spectrosc. Relat. Phenom. **5**, 985 (1974).

[2]S. Svensson, N. Mårtennson, E. Basilier, P. Å. Malmquist, U. Gelius, and K. Siegbahn, Phys. Scr. **14**, 141 (1976).

[3]J. B. West, P. R. Woodruff, K. Codling, and R. G. Houlgate, J. Phys. B **9**, 407 (1976).

[4]L. Torop, J. Morton, and J. B. West, J. Phys. B **9**, 2035 (1976).

[5]S. P. Shannon, K. Codling, and J. B. West, J. Phys. B **10**, 825 (1977).

[6]M. S. Banna, M. O. Krause, and F. Wuilleumier, J. Phys. B **12**, L125 (1979).

[7]M. O. Krause, T. A. Carlson, and P. R. Woodruff, Phys. Rev. A **24**, 1374 (1981).

[8]S. H. Southworth, P. H. Kobrin, C. M. Truesdale, D. Lindle, S. Owaki, and D. A. Shirley, Phys. Rev. A **24**, 2257 (1981).

[9]S. Southworth, U. Becker, C. M. Truesdale, P. H. Kobrin, D. W. Lindle, S. Owaki, and D. A. Shirley, Phys. Rev. A **28**, 261 (1983).

[10]B. W. Yates, K. H. Tan, L. L. Coatsworth, and G. M. Bancroft, Phys. Rev. A **31**, 1529 (1985).

[11]U. Becker, T. Prescher, E. Schmidt, B. Sonntag, and H. -E. Wetzel, Phys. Rev. A **33**, 3891 (1986).

[12]J. W. Cooper, Phys. Rev. Lett. **13**, 762 (1964).

[13]S. T. Manson and D. J. Kennedy, Chem. Phys. Lett. **7**, 387 (1970).

[14]S. T. Manson, Phys. Rev. Lett. **26**, 219 (1971).

[15]D. J. Kennedy and S. T. Manson, Phys. Rev. A **5**, 227 (1972).

[16]M. Y. Amusia, N. B. Berezina, and L. V. Chernysheva, Phys. Lett. **51A**, 101 (1975).

[17]M. Y. Amusia and V. K. Ivanov, Phys. Lett. **59A**, 194 (1976).

[18]G. Wendin and M. Ohno, Phys. Scr. **14**, 148 (1976).

[19]W. R. Johnson and V. Radojević, J. Phys. B **11**, L773 (1978).

[20]M. Y. Amusia, Comments At. Mol. Phys. **8**, 61 (1979).

[21]W. Ong and S. T. Manson (unpublished results).

[22]K.-N. Huang, W. R. Johnson, and K. T. Cheng, At. Data Nucl. Data Tables **26**, 33 (1981); and unpublished results.

[23]S. T. Manson and J. W. Cooper, Phys. Rev. **165**, 126 (1968).

[24]J. W. Cooper, Phys. Rev. **128**, 681 (1962).

[25]A. P. Lukirskii, I. A. Brytov, and T. M. Zimkina, Opt. Spektrosk. **17**, 438 (1964) [Opt. Spectrosc. (USSR) **17**, 234 (1964)].

[26]D. L. Ederer, Phys. Rev. Lett. **13**, 760 (1964).

[27]T. M. Zimkina and S. A. Gribovskii, J. Phys. (Paris) Colloq. **10**, C4-282 (1971).

[28]J. P. Connerade, Proc. R. Soc. London, Ser. A **347**, 581 (1976).

[29]J. B. West and J. Morton, At. Data Nucl. Data Tables **22**, 103 (1978).

[30]D. W. Lindle, P. H. Kobrin, C. M. Truesdale, T. A. Ferrett, P. A. Heimann, H. G. Kerkhoff, U. Becker, and D. A. Shirley, Phys. Rev. A **30**, 239 (1984).

[31]M. G. White, R. A. Rosenberg, G. Gabor, E. D. Poliakoff, G. Thornton, S. Southworth, and D. A. Shirley, Rev. Sci. Instrum. **50**, 1288 (1979).

[32]D. W. Lindle, P. A. Heimann, T. A. Ferrett, P. H. Kobrin, C. M. Truesdale, U. Becker, H. G. Kerkhoff, and D. A. Shirley, Phys. Rev. A **33**, 319 (1986).

[33]C. N. Yang, Phys. Rev. **74**, 764 (1948).

[34]D. W. Lindle, T. A. Ferrett, P. A. Heimann, and D. A. Shirley, Phys. Rev. A **34**, 1131 (1986); G. C. Angel, J. A. R. Samson, and G. Williams, Appl. Opt. **25**, 3312 (1986); J. Nordgren and R. Nyholm (private communication).

[35]T. E. H. Walker and J. T. Waber, J. Phys. B **6**, 1165 (1973).

[36]D. P. Spears, H. J. Fischbeck, and T. A. Carlson, Phys. Rev. A **9**, 1603 (1974).

[37]T. A. Ferrett, D. W. Lindle, P. A. Heimann, M. N. Piancastelli, P. H. Kobrin, H. G. Kerkhoff, U. Becker, W. D. Brewer, and D. A. Shirley (unpublished results).

[38]For example, He^{+} (2p), as in D. W. Lindle, T. A. Ferrett, U. Becker, P. H. Kobrin, C. M. Truesdale, H. G. Kerkhoff, and D. A. Shirley, Phys. Rev. A **31**, 714 (1985), and references therein.